Effect of Reinforcement Length and Distribution on Safety of Slopes

R. L. Michalowski & A. Zhao
Johns Hopkins University, Baltimore, MD, USA

ABSTRACT: An example of a reinforced slope is shown. The most crucial failure mechanism found in stability calculations is one which allows the pull-out failure mode for some reinforcement layers, and the rupture for others (mixed mode of failure). The length and distribution of reinforcement is varied to indicate potential benefits in terms of the increase in the safety factor. For the example presented, the potential increase in the safety factor due to varied length (while the total amount of geosynthetic kept constant) was found to be negligible, but a clear adverse effect occurred for some distributions of geosynthetic length and spacing.

1 INTRODUCTION

Design of the amount of reinforcement in slopes is usually done through applying the traditional limit equilibrium technique where additional terms due to reinforcement are included (for instance, Jewell, 1991; Leshchinsky and Volk, 1985; Schmertman *et al.*, 1987). This paper uses a different technique, based on the kinematic approach of limit analysis. This technique is then employed to calculate safety factors for one slope where different lengths and distribution of reinforcement are considered. The aim is to indicate the possible benefits (or the lack of) of nonuniform spacing and length of geosynthetic.

2 KINEMATIC APPROACH

This approach is presented here rather briefly since the issue central to this note is not the technique itself, but the influence of the length and distribution of geosynthetic on the critical failure modes. The kinematic approach of limit analysis was presented earlier in conjunction with the translational failure modes of reinforced slopes (Michalowski and Zhao, 1993).

Two potential failure patterns are considered here: one where the reinforced soil mass is regarded as one rigid block (Fig. 1(a)) and failure may occur due to overturning or "sliding", and the rotational mechanism (Fig. 1(b)). They both are reasonable modes of failure of a slope (wall) over a firm foundation.

The kinematical approach of limit analysis is based on the upper bound theorem which states that *the energy dissipation rate is at least as large as the rate of external forces work in any kinematically admissible failure mechanism.* Consequently, if the rate of the energy dissipation is equated to the rate of work of external forces, the load calculated will not be smaller than the true collapse load. In the present approach the factor of safety is of interest, and the method will be adjusted to yield the upper bound to the safety factor.

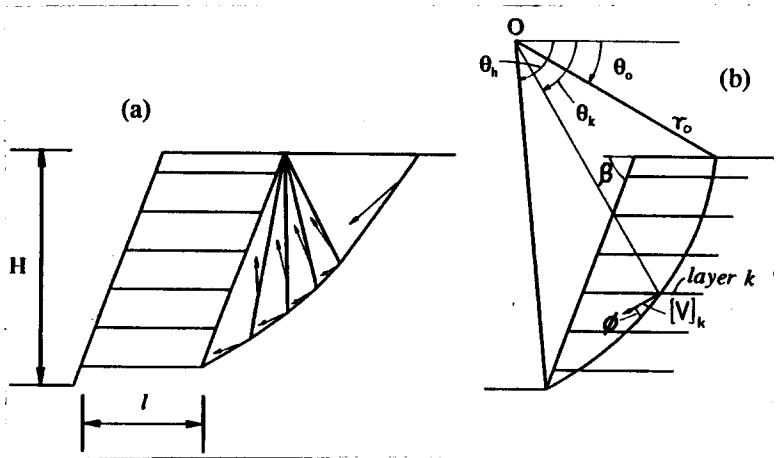

Figure 1 (a) Failure mechanism for "external stability" analysis; (b) rotational collapse pattern.

Calculations for the mechanism in Fig. 1(a) follow a standard technique (Chen, 1975). The technique for the rotational mechanism involving rupture or pull-out of reinforcement will be briefly described. The slope

considered to stand on a firm foundation and the failure surface (velocity discontinuity) passes through the toe (Fig. 1(b)). We first assume that the reinforcement is long enough so that its failure occurs in the rupture mode rather than pull-out. The fill is granular (with no cohesion), conforms to the Mohr-Coulomb failure criterion, and it obeys the associative flow rule. Hence, the energy will be dissipated during collapse of the structure only due to failure of the reinforcement

$$\dot{D} = \sum_{k=1}^{n} T_k [V]_k \sin\theta_k \qquad (1)$$

where T_k is the magnitude of the limit force in the *k-th* layer of reinforcement (tensile strength per unit length), $[V]_k$ is the magnitude of the velocity discontinuity ("velocity jump") at the rupture surface where it passes through the *k-th* reinforcement layer, and n is the number of reinforcement layers (see Fig. 1(b) for θ). The rate of work of the soil weight (work of external forces) can be calculated as

$$\dot{W} = \rho \int_v g_i V_i \, dv \qquad (2)$$

where ρ is the mass density of the soil, g_i is the gravity acceleration vector, V_i is the velocity vector, and v is the volume of the failing soil mass. The associative flow rule requires that the discontinuity velocity vector be inclined to the rupture surface at angle of internal friction φ, and the shape of the rupture surface in the rigid rotation mechanism be a log-spiral

$$r = r_0 e^{(\theta-\theta_0)\tan\varphi} \qquad (3)$$

where r_o is the radius at some initial angle θ_o. Geometrical considerations allow one to calculate the work rate in eq. (2) as

$$\dot{W} = r_o^3 \dot{\omega} \gamma \, (f_1 - f_2 - f_3) \qquad (4)$$

where $\dot{\omega}$ is the velocity about the center of rotation (rotational velocity), γ is the specific weight of the soil (ρg), and functions f_1, f_2, and f_3 are dependent on the geometry of the slope (inclination angle β), geometry of the failure surface (angles θ_o and θ_h, see Fig. 1(b)), and internal friction angle φ. These functions can be found in an earlier paper on limit analysis of slopes by Chen *et al.* (1969). For a stable slope the energy dissipation rate calculated from eq. (1) must be larger than the work rate in eq. (4) for any kinematically admissible mechanism. The factors of safety for soil and reinforcement are introduced as

$$F_s = \frac{\tan\varphi}{\tan\varphi_d}, \qquad F_r = \frac{T}{T_d} = \alpha F_s \qquad (5)$$

where φ_d and T_d are the internal friction angle and the force in the reinforcement necessary to maintain limit equilibrium. Coefficient α is a given ratio F_r/F_s. Kinematical admissibility requires that the magnitude of the velocity "jump" along the failure surface propagates according to: $[V] = [V]_o \exp\{(\theta-\theta_o)\tan\varphi\}$, and $[V]_o = r_o \dot{\omega}$. Upon substituting $\varphi_d \rightarrow \varphi$ and $T_d \rightarrow T$ in eqs. (1) and (4), and by requiring that $\dot{W} = \dot{D}$, one obtains

$$F_s = \frac{\sum_{k=1}^{n} T_k \sin\theta_k \, e^{(\theta_k-\theta_o)\tan\varphi_d}}{\alpha r_0^2 \gamma (f_1 - f_2 - f_3)} \qquad (6)$$

where T_k is the limit force in the *k-th* layer of reinforcement, and θ_k is angle θ determined for each layer of reinforcement (Fig. 1(b)). The log-spiral failure surface is determined by angles θ_0 and θ_h, and the minimum of the safety factor is sought with θ_0 and θ_h being variable. While this technique may seem, at first, to be more complicated than the traditional limit equilibrium considerations, it requires no more effort than calculations based on the moment equilibrium. Moreover, if identical failure surfaces are considered, the two methods yield identical solutions. This is not surprising, since, by the principle of virtual work, the system which is "forced" to satisfy the energy balance on the incipient mechanism must satisfy static equilibrium.

The approach described in the preceding paragraphs can be used for both reinforcement rupture and pull-out modes. In the latter, however, the force T in eq. (6) must be taken as the pull-out force (multiplied by α) rather than the tensile strength of the reinforcement. The pull-out force can be calculated approximately as

$$T^p = 2\gamma z l_e \mu \qquad (7)$$

where z is the depth of the reinforcement layer, l_e is its effective length (beyond the failure surface), and μ is the friction coefficient between the geosynthetic material and the fill. This coefficient is often calibrated as the fraction of the tangent of the internal friction angle (*e.g.*, 0.7 tan φ).

3 REINFORCEMENT LENGTH

An additional failure mechanism considered when calculating the length of reinforcement is one where no rupture of reinforcement is included. Such an analysis is often referred to as an "external stability" analysis. The collapse mechanism used here is shown in Fig. 1(a).

Rotational collapse mechanisms, as shown in Fig. 2, however, led to factors of safety lower than the mechanism in Fig. 1(a).

Calculations of the safety factor for a slope with different lengths of reinforcement were performed, and the results are presented in this section. The slope is 6.0 m high, with an inclination angle of 70°, and with the reinforcing layers spaced every 1.0 m starting at 0.5 m above the firm foundation (6 layers). The tensile strength

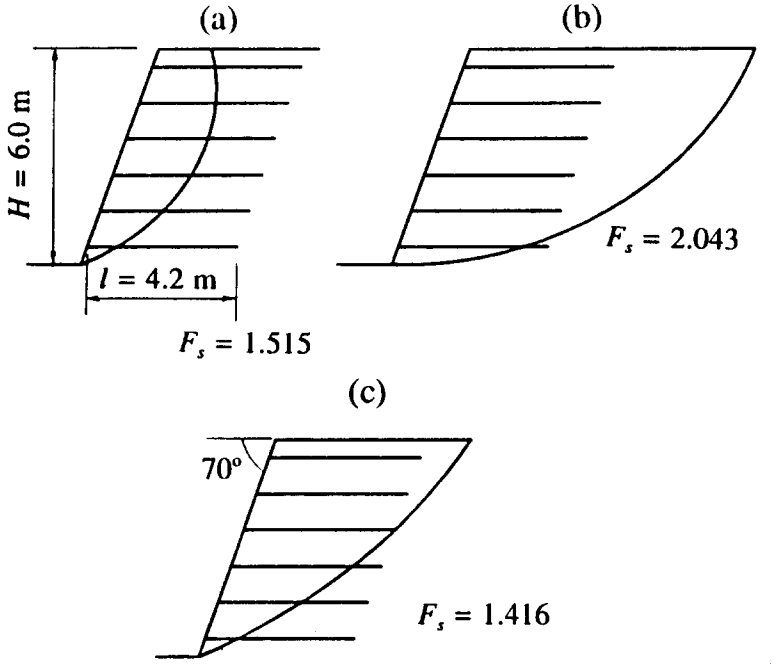

Figure 2 Failure surfaces in rotational mechanism, reinf. length $l = 0.7H$: (a) all reinforcement layers rupture; (b) pull-out or rigid; (c) mixed mode (rupture/pull-out).

of a single reinforcement layer is T = 30 kN/m. The internal friction angle of the fill is $\varphi = 35°$ (no cohesion), unit weight $\gamma = 18$ kN/m^3, and the friction coefficient between the reinforcement and the fill is $\mu = 0.7 \tan \varphi$. A requirement is imposed that the safety factor against reinforcement rupture is 1.2 times larger than that calculated for the soil, $\alpha = F_r/F_s = 1.2$. The length of reinforcement was taken as $0.7H$ (4.2 m).

Fig. 2(a) shows the failure surface for which the factor of safety becomes a minimum when all layers of reinforcement are considered to fail by rupture. This safety factor is $F_s = 1.515$. Fig. 2(b) presents a failure surface when it is required that the failure surface extends beyond the reinforcement or the reinforcement fails only by pull-out. The minimum of F_s is associated with the mechanism where only the bottom layer contributes to energy dissipation (pull-out). The change in the location of the rupture surface contributes now to a significant increase in the safety factor ($F_s = 2.043$). The most crucial mechanism is found, however, when the analysis allows the consideration of the pull-out failure mode for some reinforcement layers, and the rupture for others (mixed mode of failure) as in Fig. 2(c). The safety factor for this mechanism is $F_s = 1.416$. The "external stability" analysis (Fig. 1(a)) yields in this case $F_s = 2.104$.

When the length of reinforcement is reduced to $0.5H$ (3.0 m), the drop in the safety factor for the mixed mode failure becomes more significant, $F_s = 1.218$. The factor of safety calculated for $l = 0.5H$ and the failure mode as in Fig. 1(a) is now 1.795, still considerably larger than that in the mixed rupture/pull-out mode.

Some benefit in terms of the increase in the safety factor can be expected when the length of reinforcement is varied. Figure 3 presents the same slope as in Fig. 2; this time, however, the length of reinforcement is varied with the average length still being equal to $0.7H$ (the same amount of reinforcement). In the example the three top layers of reinforcement are lengthened while the three bottom ones are shortened. Only a small increase in the safety factor was found, however, when a non-homogeneous length of reinforcement was used. The safety factor becomes $F_s = 1.452$ when the ratio of the upper layers length to the bottom length is 1.8. When this ratio was large, a significant drop in the safety factor was noticed.

4 SPACING OF REINFORCEMENT

Spacing of reinforcement is often varied in order to gain the maximum benefit from reinforcement. The same example of the slope is used to demonstrate the effect of

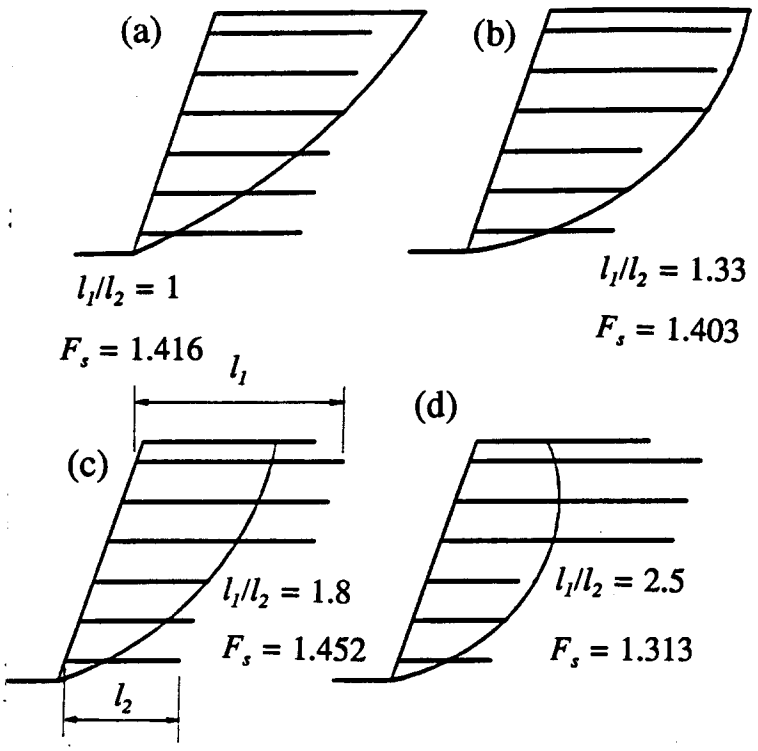

Figure 3 Failure surfaces and minimum safety factors for a slope with reinforcement of different lengths.

varied spacing. The spacing used in the example is as shown in Figs. 4(a) and 4(c). Failure mechanisms where rupture surfaces pass through the slope face above the toe must now be accounted for. Fig. 4(b) shows the safety factors calculated for uniform distribution. The magnitude of the factor of safety is marked in Fig. 1(b) at levels where the failure surface was assumed to pass through the slope face (immediately above reinforcing inclusions). For the homogeneous spacing of reinforcement, the safety factor reaches a minimum for the mechanism passing through the toe. The non-homogeneous distribution produces a very small increase in F_s against toe failure, but a failure surface above the toe now yields a lower safety factor (F_s = 1.379). Clearly, varied spacing was of no benefit.

5 CONCLUDING REMARKS

Reinforcement length has a clear effect on the potential failure mode. Only for reinforcement that is long with respect to the slope height can the reinforcement be expected to fail all in the rupture mode. Calculations for the specific example indicate that including both rupture and pull-out modes is crucial to estimating the true safety factor (minimum one). The "external stability" analyses may, in some cases, significantly overestimate the safety factor. Using a non-uniform length of reinforcement was not found to be a very effective way of increasing the safety factor. Non-uniform length and spacing of reinforcement may lead to an adverse effect, however.

There may not be as great a benefit from nonuniform length and spacing of reinforcement as generally conjectured. This conclusion is drawn from limited calculational results, and further study is needed before more general conclusions are drawn.

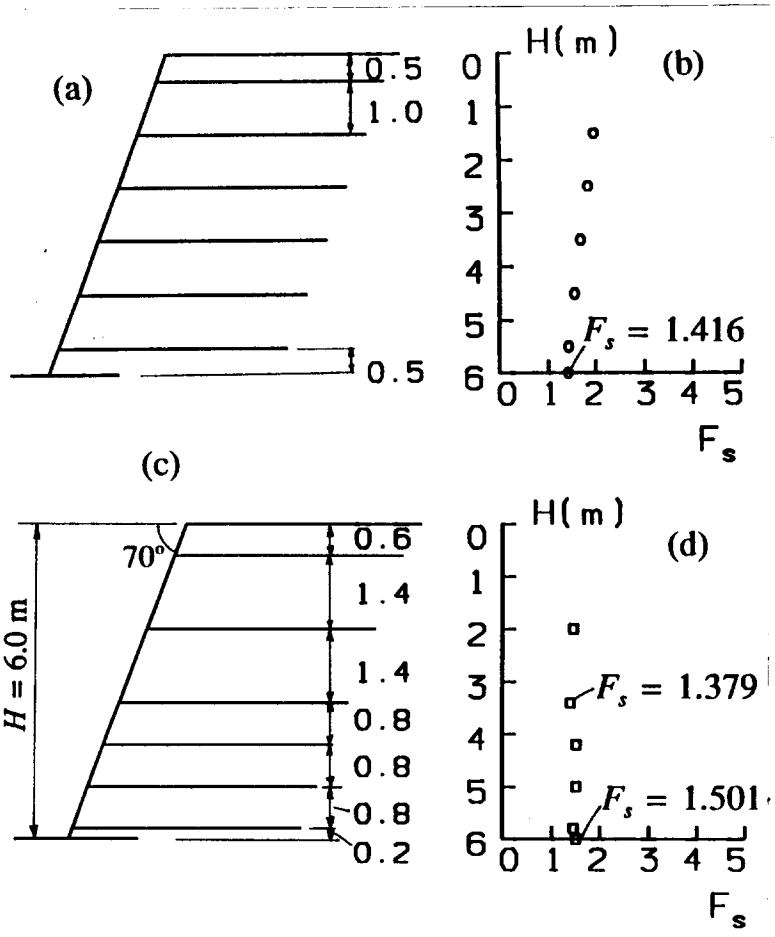

Figure 4 Factors of safety from "top-down" calculations: (a, b) uniform spacing; (b, c) non-uniform spacing.

Acknowledgement

The results presented are based upon work supported by the National Science Foundation under Grant No. MSS9301494.

6 REFERENCES

Chen, W.F. (1975). *Limit Analysis and Soil Plasticity.* Amsterdam: Elsevier.

Chen, W.F., Giger, M.W. and Fang, H.Y. (1969). On the limit analysis of stability of slopes. *Soils and Foundations*, **9**, No. 4, 23-32.

Jewell, R.A. (1991). "Application of revised design charts for steep reinforced slopes." *Geotextiles and Geomembranes*, 10, 203-233.

Leshchinsky, D. and Volk, J.C (1985). "Stability charts for geotextile-reinforced walls." *Transportation Research Record*, 1131, 5-16.

Michalowski, R.L. and Zhao, A. (1993). "Failure criteria for homogenized reinforced soils and application in limit analysis of slopes." Proc. *Geosynthetics '93*, Vancouver, Industrial Fabrics Association Int., Vol. 1, 443-453.

Schmertmann, G.R., Chouery-Curtis, V.E., Johnson, R.D. and Bonaparte, R. (1987). "Design charts for geogrid-reinforced soil slopes." Proc. *Geosynthetics '87*, New Orleans, Industrial Fabrics Association Int., Vol. 1, 108-120.